Journal of Molecular Liquids 224 (2016) 832–841

Contents lists available at ScienceDirect

Journal of Molecular Liquids

journal homepage: www.elsevier.com/locate/molliq

Modeling of adsorption kinetic and equilibrium isotherms of naproxen onto functionalized nano-clay composite adsorbent

Lida Rafati [a,e], Mohamad Hassan Ehrampoush [a,e], Amir Abbas Rafati [b], Mehdi Mokhtari [a], Amir Hossein Mahvi [c,d,*]

[a] Environmental Sciences and Technology Research center, Department of Environmental Health Engineering, Shahid Sadoughi University of Medical Sciences, Yazd, Iran
[b] Department of Physical Chemistry, Faculty of Chemistry, Bu-Ali Sina University, P.O. Box 65174, Hamedan, Iran
[c] Center for Solid Waste Research (CSWR), Institute for Environmental Research (IER), Tehran University of Medical Sciences, Tehran, Iran
[d] Department of Environmental Health Engineering, School of Public Health, Tehran University of Medical Sciences, Tehran, Iran
[e] Research Center for Food Hygiene and Safety, Shahid Sadoughi University of Medical Sciences, Yazd, Iran

ARTICLE INFO

Article history:
Received 23 August 2016
Received in revised form 11 October 2016
Accepted 12 October 2016
Available online 19 October 2016

Keywords:
Adsorption
Kinetic models
Equilibrium isotherm models
Naproxen
Batch study

ABSTRACT

In this research, nano-clay was firstly modified with β-cyclodextrin and polymerized by polyvinylpyrrolidone (PVP) to provide more surfaces for higher adsorption. The adsorption process as batch study was investigated under the experimental conditions affecting some parameters such as pH, contact time, concentration of naproxen and the amount of adsorbent for adsorption efficiency. Then, the adsorption kinetic and equilibrium isotherms were also studied. The results showed that the adsorption was influenced by some factors such as initial concentration of naproxen, the amount of adsorbent and solution's pH. The optimum values of adsorbent dosage, contact time, initial naproxen concentration and pH were evaluated as 1 g, 120 min, 10 mg/l and 6, respectively. Also, the maximum efficiency of adsorption was achieved 92.2%. The equilibrium constant was studied with 9 more common isotherm models, and among them, all isotherm models could well describe the adsorption of naproxen on the modified nano-composite except Langmuir and Tempkin models that show large deviation from experimental data. This was confirmed by investigating the results of error function analysis. Moreover, it was indicated that the adsorption follows Elovich kinetic model. Based on the obtained results, it can be stated that the adsorption method using the modified nano-composite is an efficient, facile and reliable method for the removal of naproxen from aqueous solutions.

1. Introduction

Pharmaceutical products which are essential elements and integral part of modern life are used to treat human and animal diseases. Nevertheless, the impacts of pharmaceutical pollutants on the environment are evident [1–7]. Naproxen belongs to non-steroidal anti-inflammatory drugs (NSAIDs) which can reduce certain hormones causing inflammation and pain [7–9]. NSAIDs are among the most widely used medicines that are produced and consumed in large quantities [10]. Most of pharmaceutical compounds, after use, are discharged into the sewer via urine and feces without changing or as decomposed byproducts, which affect human health, directly and indirectly by entering the food chain [11,12].

Tertiary and advanced treatments in the aquatic environment, such as adsorption technology using mineral adsorbents, are necessary to remove pharmaceutical contaminants from the environment, since conventional treatment systems such as coagulation, sedimentation and filtration are only able to remove 25% of these substances [13]. In recent years, adsorbent materials with nanostructures or nano-composites have been increasingly used to remove contaminants [14–31].

The objective of this work is to synthesis and characterization of a new polymer-clay composite adsorbent, functionalized with β-CD groups. Also, a comparison of the adsorption properties of functionalized polymer-clay composite to those of clay, aiming for future applications in water and wastewater treatment. The adsorbents for naproxen were prepared using nano-clay (Cloisite 15A) as starting materials for surface modification. The effects of various parameters such as contact time, the amount of adsorbent, initial concentration and pH were studied on nanocomposite adsorbent. Then, adsorption method was used to remove naproxen from water and wastewater and obtained experimental data were fitted with nine different adsorption isotherm models. Also, the kinetics of adsorption was studied by four models. Finally, error functions analysis was applied for experimental data.

* Corresponding author at: Center for Solid Waste Research (CSWR), Institute for Environmental Research (IER), Tehran University of Medical Sciences, Tehran, Iran.
E-mail address: ahmahvi@yahoo.com (A.H. Mahvi).

http://dx.doi.org/10.1016/j.molliq.2016.10.059
0167-7322/

2. Materials and methods

2.1. Materials

Cloisite 15A was used in this study that was purchased from Neutrinos Company. Naproxen pure was prepared from pharmaceutical company Alborz bulk (Iran) as a gift. All chemicals were purchased from Merck with analytical grade. Standard solutions of the naproxen were prepared by dissolving an appropriate weight of pure naproxen salt in distilled water. The working solution of naproxen (3, 5 and 10 mg/l) were prepared by diluting the stock solution in distilled water. The batch method was applied to study the adsorption of naproxen on strong nano clay composite. All experiments were performed at room temperature and the effect of parameters such as pH, initial concentration of naproxen, contact time and the amount of adsorbent on removal efficiency were investigated. The final naproxen concentration in the effluent was determined by the UV–Vis spectrophotometric method using UV/VIS spectrophotometer (PG-Instruments Ltd) at 230 nm. Finally, kinetics parameters and adsorption isotherms were studied.

2.2. Preparation of nanocomposite briefly

The used nanocomposite adsorbent in this research was prepared as follows: firstly, monotosyl-β-cyclodextrin (Ts-βCD) was synthesized and prepared. β-CD (18 g) was dissolved in dry pyridine (100 mL), and then *p*-toluenesulfonyl chloride (2.5 g) was added to this solution. The reaction mixture was stirred well in the temperature range of 2–4 °C for about 8 h, and then the solution temperature reached to room temperature and the reaction mixture was kept for two days at this temperature. After this step, the solution was concentrated under the reduced pressure, and then, diethyl ether was added. The obtained white solid product was washed with acetone, and then dried under vacuum condition at 60 °C [32–34].

To modify the substance Cloisite 15A, with 3-aminopropyltriethoxy silane (APTS), substance Cloisite 15A (0.5 g) was dissolved in a mixture of 25 ml of toluene, and the mixture was put in an ultrasonic bath for 30 min and extremely stirred under reflux condition for 40 min. Then, APTS (2.5 mol) was gradually added. The reaction was heated under nitrogen atmosphere for 3 h. The obtained compound was washed with water and acetone several times to remove ever impurities, and then dried in an oven at 150 °C for 2 h.

After conducting the above steps, to modify the substance β-CD with NH_2-Clay which is the main structure of nanocomposite, compound NH_2-Clay (2 g) was added to dimethyl formamide (DMF) (50 mL), and extremely stirred for 7 h. Then, compound Ts-βCD (0.25 g) which was separately dissolved in DMF (10 mL) was added to the mixture. The obtained mixture was heated at 60 °C at pH = 7–8 under nitrogen atmosphere, and then the resulting product was washed with DMF and acetone to remove ever impurities, and dried in an oven 24 h.

2.3. Adsorption experiments

Stoke solutions of naproxen were prepared in different concentrations in one-liter baker as a batch reactor, and then a certain amount of adsorbent was evaluated according to the ratio of the adsorbent to the pollutants (*R*) (Eq. (1)), including 12.5, 25, 50 and 100 in a batch system and then mixed by magnetic stirring at a speed of 300 rpm. Optimal *R*s are obtained corresponding to the less remaining naproxen. Optimal % *R* was calculated from Eq. (1):

$$\%R = \frac{C_a}{C_0} \times 100 \tag{1}$$

where C_a is the amount of adsorbed naproxen (difference in naproxen concentration in the aqueous solution before and after sorption) and C_0 is the initial concentration of naproxen.

The adsorbent adsorbate uptake, q_t (mg/g) was calculated by Eq. (2):

$$q_t = \frac{(C_0 - C_t)V}{m} \tag{2}$$

where C_0 and C_t, are the initial concentration of naproxen and naproxen concentration at a time of (t) in terms of mg/l respectively, V is volume of the solution (L) and m is the amount of adsorbent (g) [35–37].

2.4. Determination of pH optimized and pH point of zero charge $_{(ZPC)}$

The effect of pH (5–9) on the removal efficiency was evaluated after determining the optimum *R*s and contact times. The pH range between 5 and 9 was adjusted by 0.1 N NaOH and HCl using pH meter (from Metrohm Company, model 827).

The pH_{ZPC} is a point of pH in which the surface charge of adsorbent is equal to zero. The importance of this point is to determine the properties of adsorbent surface. In this way, at a pH higher than pH_{ZPC}, the adsorbent surface has a negative charge so that ions with opposite charge (positive ions) are easily adsorbed. Also, at lower pH, the surface charges are positive, and ions with negative charges are adsorbed more quickly [38–40]. To determine the pH_{ZPC} of the studied adsorbent, 50 mL of potassium nitrate solution (0.01 M) was added to seven Erlenmeyer flasks, and initial pH of each flask was adjusted between 2 and 12 using 0.1 N of HCl or NaOH solutions. Then, the prepared adsorbent (0.1 g) was added to each flask, and the mixtures were stirred for 24 h. After measuring the final pH of each solution, the final pH versus initial pH was plotted, and pH_{ZPC} was determined.

2.5. Equilibrium adsorption experiment

In this study, Langmuir, Freundlich, Tempkin, Redlich-peterson (R-P), Sip, Radke–Prausnitz, Fritz–Schlunder, Toth and Khan adsorption isotherms were evaluated and all of the equations are listed in Table 1.

2.6. Kinetic models

Equations of adsorption kinetic are the methods of analysis for adsorption reaction; the most widely used of these models include pseudo-first order, pseudo-second order, Interparticle Diffusion and Elovich kinetic equations which were used in this study.

2.6.1. Pseudo-first-order model (Lagergren)

Eq. (3) shows the pseudo-first order model [41–44]:

$$Ln(q_e - q_t) = Lnq_e - k_1 t \tag{3}$$

where q_e indicates the ratio of equilibrium uptake of naproxen on adsorbent as mg/g, q_t is adsorption of naproxen on adsorbent at the time of (t) and k_1 is rate constant for pseudo-first-order based on g mg^{-1} min^{-1}. If the curve obtained is linear, adsorption kinetics follows this model.

2.6.2. Pseudo-second-order model

This model is based on the hypothesis that the rate of used adsorbent sites is proportional to the square of the number of sites involved. Eq. (4) is the linear form of this model [45–51]:

$$\frac{t}{q_t} = \frac{1}{k_2 {q_e}^2} + \frac{t}{q_e} \tag{4}$$

where k_2 (g mg^{-1} min^{-1}) indicates overall rate constant of pseudo-second-order. A plot of t/q_t versus t shows a straight line with an intercept and slope of $1/k_2q^2$ and $1/q_e$, respectively.

Table 1
Isotherm models as nonlinear forms.

Isoterm model	Equation
Langmuir	$q_e = \frac{q_m k_L c_e}{1 + k_L c_e}$
Froundlich	$q_e = k_F C_e^{1/n}$
Tempkin	$q_e = (\frac{RT}{b_T})\ , \ln(k_T C_e)$
Fritz–Schlunder	$q_e = \frac{q_{mFS} k_{FS} C_e}{1 + q_m C_e^{mFS}}$
Radke–Prausnitz (R-P)	$q_e = \frac{q_{mRMPI} k_{RPI} C_e}{(1 + k_{RPI} C_e)^{mRPI}}$
Redlich-peterson (P-R)	$q_e = kC_e/(1 + \alpha_R C_e^{\beta})$
Sips	$q_e = q_m k C_e^{\frac{1}{n}}/(1 + kC_e^{\frac{1}{n}})$
Toth	$q_e = \frac{q_{mT} C_e}{(1/k_T + C_e^{mT})^{1/mT}}$
Khan	$q_e = q_m \frac{b_k C_e}{(1 + b_k C_e)^{n/k}}$

2.6.3. The Elovich

The Elovich or Roginsky–Zeldovich equation is expressed as follows [52–57]:

$$q_t = \frac{\ln a_e b_e}{b_e} + \frac{1}{b_e} \ln t \tag{5}$$

where a_e, initial adsorption rate (mg/g min) and b_e (g mg^{-1}) are the parameters of the Elovich rate equation obtained from the linear regression analysis of the q_t versus ln*t*.

2.6.4. Intraparticle diffusion model

This model equation is expressed as follows [58–60]:

$$q_t = k_p t^{1/2} + C \tag{6}$$

where, *C* is the y-intercept and k_p (mg/g $min^{-1/2}$) is the rate constants of intra-particle diffusion.

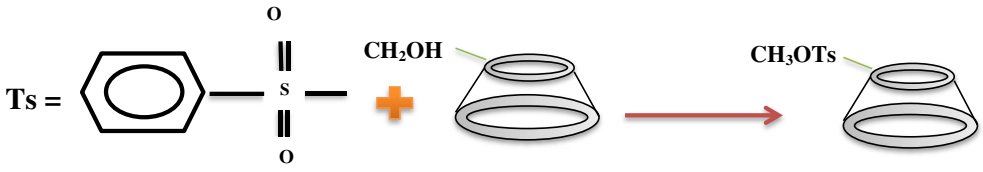

Step 1: ***Tscl +β-CD***

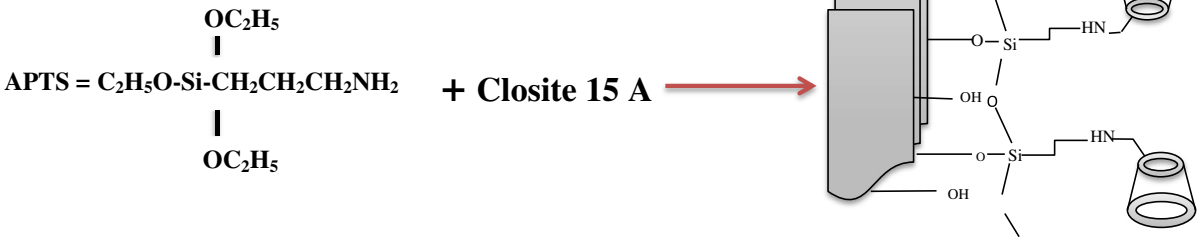

Step 2: ***APTS modification***

Step 3: ***APTS+ Clay + β-CD + PVP***

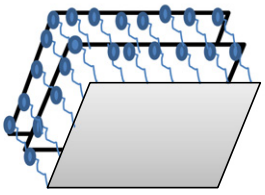

Scheme 1. Preparation procedure for fabricating β-CD, APTS and PVP bonded nano Cloisite 15A.

3. Results and discussion

3.1. Preparation of adsorbent

Scheme 1 shows the synthesis procedure for nanocomposite preparation. FT-IR spectra of raw materials as well as prepared nanocomposite are depicted in Fig. 1. As can be seen from the FT-IR spectrum of nanocomposite, the observed peak at 1058 cm^{-1} is the same peak in Cloisite 15A spectrum while that peak is absent in β-CD and PVP spectra. On the other hand, observed peaks at 1058, 529, and 467 cm^{-1} on the silylated Cloisite 15A spectrum indicate the Si—O group.

Peak at 1696 cm^{-1} (C═O stretching vibration) is present in PVP and nanocomposite spectra but it is absent in β-CD. Cloisite 15A has a peak in the area of 3645 cm^{-1} which corresponding to the O—H free groups. The peaks in the range of 2932 and 2861 cm^{-1} illustrate the modified alkyl chain in clay. The different peaks of the obtained nanocomposite are as follows: peaks of CH_2 (2932, 2861 cm^{-1}) and Si—O (1058, 529, and 467 cm^{-1}), which are related to the polymer and clay, respectively.

In this research, the SEM analysis was employed to determine the morphology of nanocomposite surface (Fig. 2). The SEM images of starting material and nanocomposite, as depicted in Fig. 2a and b, respectively, shows the difference between the morphology of layers before and after intercalation. The spaces between the layers prove the presence of polymer in these spaces.

The XRD patterns of nanocomposite and starting materials are depicted in Fig. 3. The properties of these patterns include: a) a peak at $2\theta = 7.3°$, is corresponding to (001) crystallographic plane of clay and the distance of clay layer is equal to 1.21 nm; b) peak at $2\theta = 2.9°$, which related to the MMT layers is correspond to 3.04 nm layer distances for nanocomposite layers. In comparison with clay, increased in interlayer spacing is due to insertion of polymer chain between clay layers [61,62].

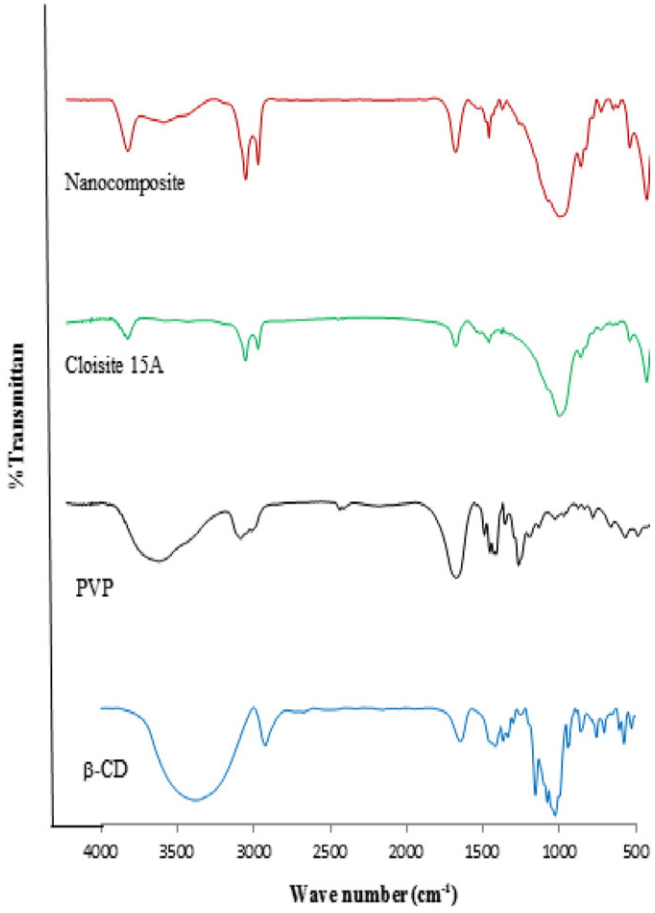

Fig. 1. The FT-IR spectra of the cyclodextrin, PVP, Cloisite 15A, CD-Clay and nanocomposite.

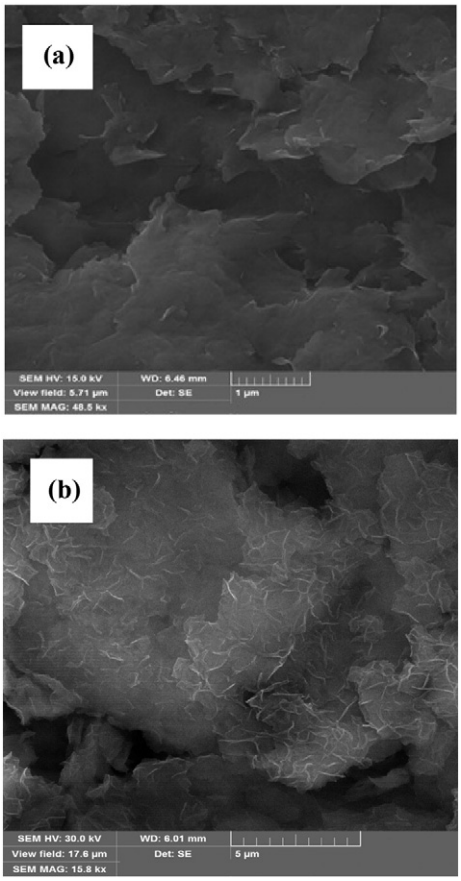

Fig. 2. SEM images of (a) Cloisite 15A and (b) nanocomposite.

3.2. Adsorption analysis

To determine the amount of optimized *R* [63] and to find the maximum adsorption of naproxen on the adsorbent as a function of *t*, some experiments were carried out. In this regard, 10 mg/l of naproxen with different amounts of adsorbent was investigated at optimized pH of 6 (Fig. 4, typically). $R = 12.5$ was chosen as the optimized level with contact time of 120 min and highest concentration of naproxen removal, as well. The optimized level of adsorbent/adsorbate was selected

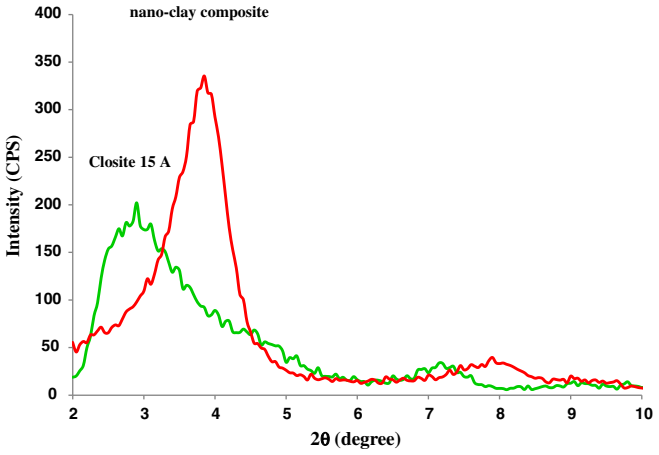

Fig. 3. XRD patterns of Cloisite 15A and nanocomposite.

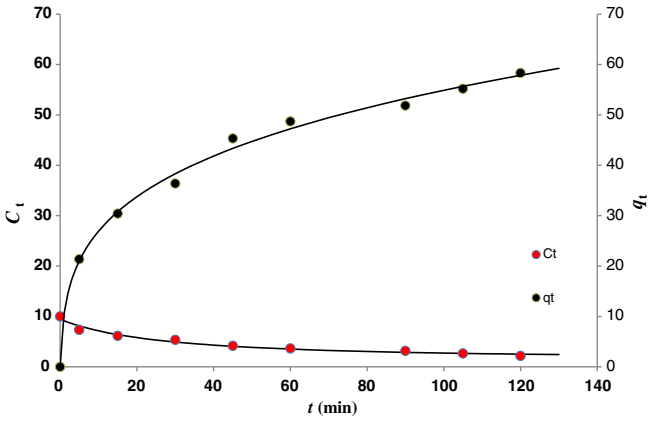

Fig. 4. Adsorption of naproxen on nano clay composite at different R values: ($R = 12.5$, $C_0 = 10$ mg/l, amount of adsorbent = 0.125 (typically)).

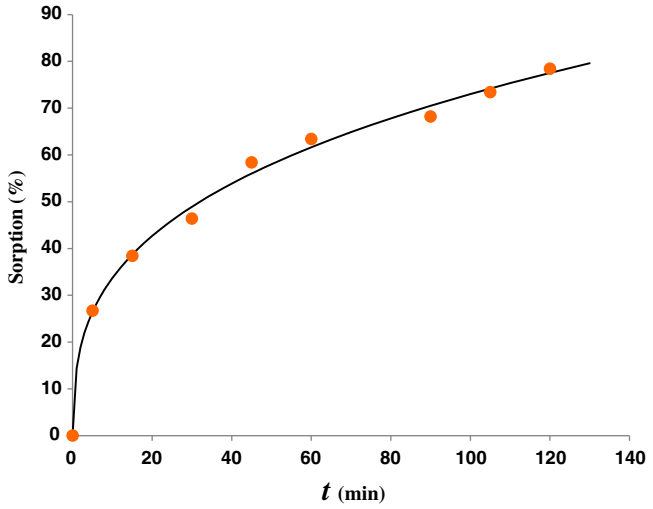

Fig. 5. Effect of time for removal of naproxen on nano clay composite adsorbent.

for all the experiments. As shown in Fig. 4, according to the small amounts of the used adsorbent (0.125 g), the minimum rate of naproxen uptake was in the first 5 min, and after a while, the adsorption rate was considerably increased. At $t = 120$ min, it reached the lowest amount of naproxen at an optimized level of adsorbent/pollutant of $R = 12.5$. It shows that the amount of adsorbent in the solution should be 12.5 times the adsorbent for the 10 mg/l naproxen to reach the lowest amount of naproxen. According to this diagram, the optimized contact time is 120 min. However, by increasing the time, the remaining amount of naproxen would reduce, but the increase in time would raise the costs of facilities and system steering. Also, Fig. 5 shows the variation of the naproxen uptake on nanocomposite adsorbent versus time at pH 6. As you can see, maximum uptake for nanocomposite was obtained at 120 min and the removal of naproxen was increased when the increased time. Therefore in this research, the optimized time was considered as 120 min [63] according to the absent of any standard defined for naproxen [64,65].

Performance of new nano-composite adsorbent was compared with some other adsorbents previously reported for removal of naproxen in Table 2.

3.2.1. The effect of pH and pH_{zpc}

Since the solution's pH affects the surface charge of adsorbent and ionization degree, the effect of solution's pH in the range of 5 to 9 on the naproxen removal by the use of nano-composite adsorbent was studied at room temperature. Fig. 6 shows the effect of pH on the adsorption process of naproxen. Also, pH_{ZPC}, which important in the interpretation of results related to pH, was determined as depicted in Fig. 7. As shown, the increase of pH up to 6 increased the amount of naproxen removal, and after that it is decreased. At pH 6, the removal efficiency was obtained as 90%, so this pH was used as the optimized pH in the experiments. On the other hand, pH has a great effect on the equilibrium constant (K_e). Therefore, it can be considered as comparative measure of the efficiencies of different adsorbents. The amount of pH can be proposed based on the type of the adsorbed compounds and mechanism of the applied adsorbent.

3.2.2. The effect of adsorbent dose

The dependence of naproxen adsorption on the amount of adsorbent was studied at the optimized pH (pH 6) which was investigated the previous section. The results are presented in Fig. 8. From this figure it is evident that at a constant initial naproxen concentration, the increase of adsorbent dose increases the efficiency of naproxen adsorption. Hence, by increasing the dose of adsorbent from 0.125 to 1 g/l, the maximum efficiency of adsorption is increased from 78.4 to 92.2% since enhancement of the adsorbent amount leads to increase in the adsorption active sites on the adsorbent which are available for naproxen ions. Also,

Table 2
Comparison of our developed nano-composite adsorbent performance with some recently reported adsorbents for removal of naproxen.

Adsorbent	Adsorption conditions	% removal	Maximum adsorption capacities	Reference
Amberlite XAD-7	Initial concentration (25–75 ppm), adsorbent dose (1–3 g/l), stirring rate (80–240 rpm), pH (2–9) and temperature (20–60 °C)	60%		[66]
Granular Activated Carbon (GAC)	Initial concentration = 500 ng/l, adsorbent dose = 23 g and EBCT = 2.6 min	90%		[67]
Molecularly Imprinted Polymer (MIP)	Initial concentration = 20 mg/l, adsorbent dose = 50 mg, extraction time = 10 min and pH = 4.6	–	1.25 mg/g	[68]
Olive waste cakes	Initial concentration (10 = mg/l), adsorbent dose = 0.3 g, T = 25 °C and pH = 4.12	70.07%	–	[69]
Magnetic activated carbon (M-AC)	Initial concentration = 10 mg/l adsorbent dose = 10 mg, T = 293 K and pH 5	87.79%	–	[70]
Fe3O4 nanoparticles on multi-walled carbon nanotubes (MWCNTs)	Initial concentration = 10 mg/l, adsorbent dose = 10 mg, T = 293 K and pH 3	67.20%	–	[70]
MIL-100-Fe	Initial concentration = 10 mg/l, adsorbent dose = 50 mg, T = 25 °C, contact time = 10 min–12 h and pH = 4.5	–	88 mg/g	[71]
SBA-15	Initial concentration = 10 mg/l, T = 25 °C, low pH and neutral pH	–	0.45 μmol/g and 0.69 μmol/g	[72]
WA11Zn5	Initial concentration = 100 mg/l, adsorbent dose = 0.1, pH 5.82, contact time = 1 h and T = 25, 37, 50 °C	–	49.69, 49.75, 49.76 mg/g	[73]
Functionalized nano-clay composite	Initial concentration = 10 mg/l, adsorbent dose = 1 g, contact time = 120 min, T = 25 °C and pH = 6	92.2%		The present study

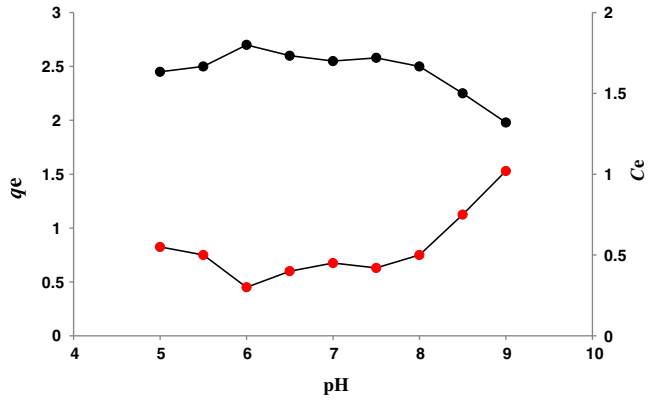

Fig. 6. Effects of pH for removal of naproxen using nano clay composite.

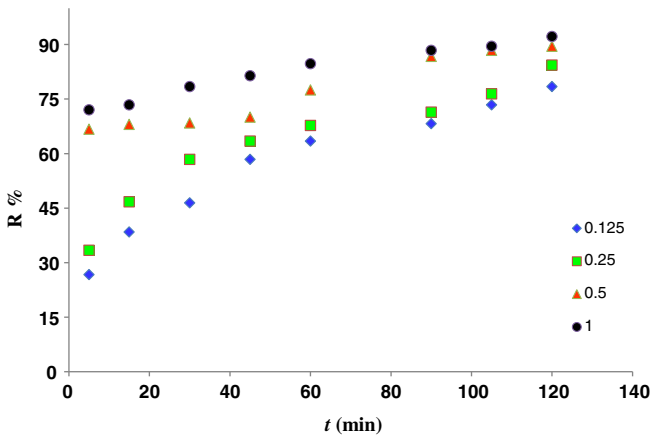

Fig. 8. Effects of adsorbent dose for removal of naproxen on nano clay composite.

Fig. 8 shows that the increase of adsorbent amount results in a decrease of the adsorption equilibrium time. This is because of two reasons: the first reason is that increasing adsorbent's dose increases the collision of adsorbate with the adsorbent particles. Consequently, the adsorption rate increases and equilibrium time decreases. The second reason is that by increasing the adsorbent dose (or decreasing the concentration of solution), the second step of kinetic adsorption process (formation of a boundary layer around the adsorbent which limits the adsorption) becomes gradually ineffective, the adsorption rate increases, and the equilibrium time decreases [74]. As can be seen from the results, this adsorbent shows a high adsorption rate at initial contact time and it was considered as a fast adsorbent so that for a typically sample with 1 g of adsorbent, 72% of naproxen was removed after $t = 5$ min ($C_0 =$ 10 mg/l).

3.2.3. The effect of initial concentration

The effect of C_0 for removal of naproxen on the modified nanocomposite adsorbent is depicted in Fig. 9. The effect of different concentration of naproxen on the adsorption uptake quantities in different times showed that the adsorption equilibrium capacity of the modified nanocomposite increases for naproxen adsorption by increasing the initial concentration of naproxen. Also, the adsorption kinetic of naproxen contains two steps: in the first one, naproxen adsorption takes place quickly, and in the second step, the adsorption is slower and finally it reaches the equilibrium point. The high rate of naproxen adsorption in the first step is related to the presence of adsorption active sites on the adsorbent which can adsorb the naproxen molecules quickly. However, the number of these adsorption active sites gradually decreases with increase in the adsorption time and the number of naproxen molecules adsorbed on the adsorbent, as well [75]. As a result, the adsorption rate significantly decreases and leads to beginning of the second step of adsorption. Furthermore, it is noteworthy that the adsorption active sites are placed on the surface and interior part of the adsorbent. So, at the beginning of the adsorption process, all these sites are ready for adsorption but surface sites are easily available for naproxen molecules and have more chance to have contact with naproxen ions. Therefore, this increases the adsorption rate, but gradually, through the saturation of surface and external sites, the adsorption continues via the internal adsorption sites and it causes the slow rate of adsorption. However, it does not mean that at the beginning of the adsorption process, the deeper sites of adsorbent are not involved in the adsorption. In fact, all sites are involved in the adsorption process but in the first phase, the adsorption rate is controlled by the surface sites of adsorbent. Also, increase in the adsorption capacity by enhancing the naproxen concentration is due to the collision of naproxen molecules with the adsorbent surface [76].

3.3. Adsorption isotherms

Adsorption isotherm is one of the significant factors in the design of adsorption process. In fact, adsorption isotherm explains how the adsorbent and adsorbate substance interact with each other. So, it is considered as a main factor for the determination of adsorbent capacity and optimizing the use of adsorbent. Therefore, the isotherm can provide

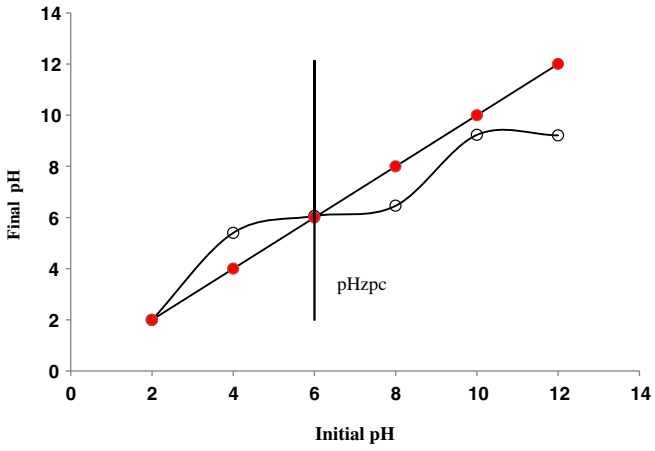

Fig. 7. Determination of pH_{ZPC} based on initial pH versus final pH.

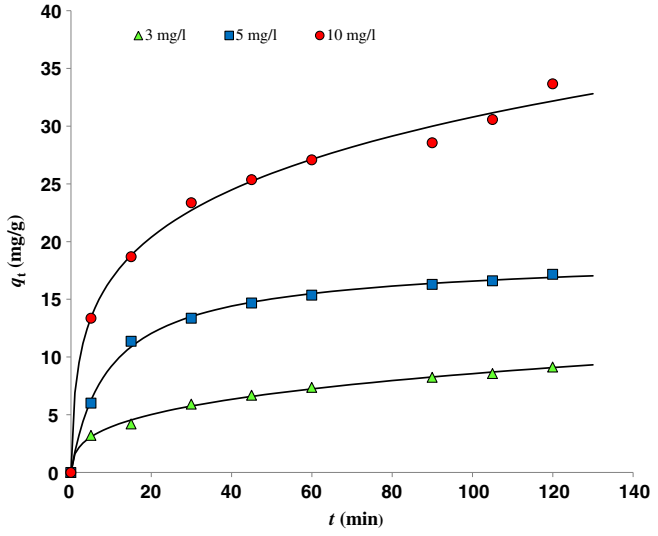

Fig. 9. Effects of initial concentration for removal of naproxen on nano clay composite.

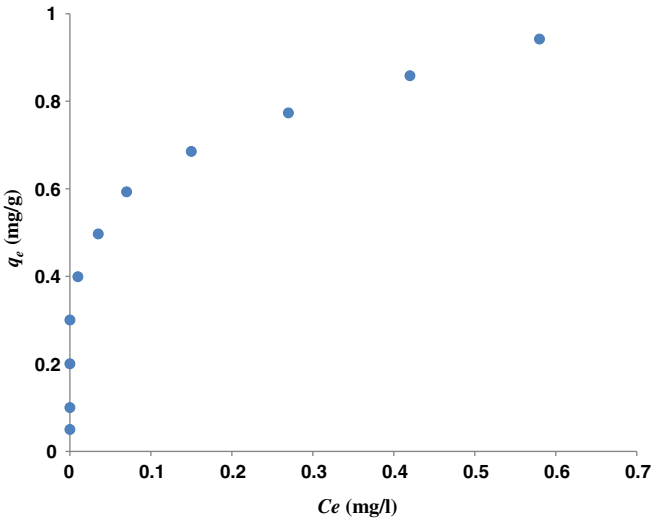

Fig. 10. Equilibrium adsorption of naproxen on nanocomposite (typically).

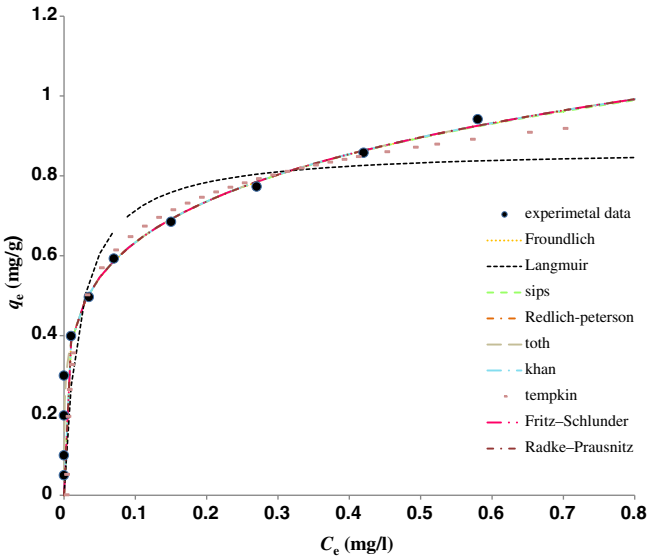

Fig. 11. Fitting data with three parameters isotherm models (typically).

some information on the maximum capacity of adsorbent for naproxen adsorption which is useful in the design of adsorption processes. In this study, the adsorption behavior of naproxen on the nanocomposite, in different concentrations of naproxen was studied. Nine isotherms were used for the explanation of adsorbent ability in the experiments. Fig. 10 shows a typical adsorption isotherm in a specified condition. As seen, the equilibrium adsorption uptake on the adsorbent increases significantly by increasing the naproxen concentration. This indicates that the adsorption on the adsorbent is a diffusion process [17]. By increasing C_0, the equilibrium adsorption uptake of the adsorbent was increased. Hence, the adsorption caused by mass transfer increases with increase in the C_0 [63]. As shown in Fig. 10, the adsorption capacity of naproxen tends to a constant trend which shows that all active sites on the adsorbent are completely filled with naproxen.

For extract isotherm model parameters, we use a nonlinear regression program for fitting data. The obtained fitting data as well as isotherm equations are summarized in Table 3. Also, the graphical representations of some models are presented in Fig. 11.

Table 3
Isotherm parameters for various common adsorption isotherms for the adsorption of naproxen onto nanocomposite adsorbent.

Isoterm model	Constants	Parameter values
Langmuir	q_m (mg/g)	0.8689
	k_L	45.9352
Froundlich	k_F	1.0410
	1/n	0.2155
Tempkin	β (j/mol)	1.1689
	k_{Te}	0.0765
Fritz–Schlunder	q_{mFSS} (mg/g)	49.4346
	k_{FS}	1.0411
	m_{FS}	0.7845
Redlich-peterson (P-R)	K_R	8.2890×10^7
	α_P	7.9617×10^7
	β	0.7845
Radke–Prausnitz (R-P)	q_{MRP}(mg/g)	0.0862
	k_{RP}	1.05433×10^5
	m_{RP}	0.7846
Sips	q_m (mg/g)	23.1575
	1/n	0.2217
	k_s	0.0469
Toth	q_m (mg/g)	1.0410
	k_{T0}	7.8814
	m_T	0.3682
Khan	q_m (mg/g)	0.0862
	b_K	1.05431×10^5
	$n/_k$	0.7846

3.4. Adsorption kinetics

The kinetics of adsorption is important for better understanding of the adsorption dynamic of adsorbate. Thus, kinetic parameters play a significant role in the design and modeling of the adsorption process, and as anticipant's models, they can provide some information on the number of molecules adsorbed during the adsorption process. This information can be used to design big systems. Experimental data of the adsorption kinetic of naproxen on the nanocomposite adsorbent was calculated using Eq. (2). In this work, four kinetic models i.e. pseudo-first-order [45], pseudo-second-order [52], Ellovich [55] and Intraparticle diffusion models [58] were used.

All the parameters obtained by kinetic models are presented in Table 4. Fig. 12 illustrates the comparison of experimental points with the fitted data. Among these four different models, it was indicated that Ellovich model showed good consistency with experimental data.

3.5. Non-linear error function analysis

Eight error functions including: residual root mean square error (*RMSE*), the coefficient of determination (R^2), correlation coefficient (r), the sum of the square of the error (*SSE*), the sum of the absolute error (*SAE*), average relative error (*ARE*), nonlinear chi-square (χ^2) and the average relative standard error (*ARS*) were used to verify the model for the adsorption system. All of the error function equations are listed in Table 5.

Table 4
Different kinetic models were obtained by the value of parameters.

Kinetic models	Parameters	Value
Pseudo-first-order	k_1	0.0835
	q_{e1}	27.4376
	r^2	0.9385
Pseudo-second-order	k_2	0.0037
	q_{e2}	30.6458
	r^2	0.9777
Elovich	α	11.2740
	β	0.1849
	r^2	0.9944
Intra-particle diffusion	k_{ad}	2.4440
	C_i	5.9860
	r^2	0.8950

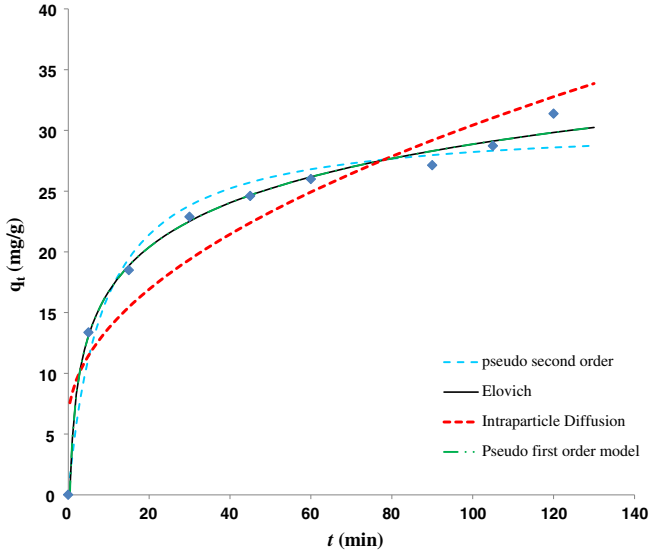

Fig. 12. Data fitting with the pseudo-first order, pseudo- second order, Elovich, Intraparticle diffusion and experimental data for removal of naproxen on nano clay composite.

Table 6 shows the results of error functions for different isotherms. In each condition, the best curve fitting is corresponding to the lower error function value. According to the results in Table 6 and comparing error functions of the adsorption isotherms, the highest correlation and the lowest error were achieved for Froundlich, Fritz–Schlunder, Redlich-peterson, Radke–Prausnitz, Sip, Toth and Khan isotherms which indicates that these models are the best fitted models for experimental data of naproxen adsorption on the adsorbent.

4. Conclusion

In this research, the functionalized nanocomposite was used as a strong adsorbent for the removal of naproxen from the aqueous solutions. First, adsorbent was provided and synthesized. Then, the behavior of this adsorbent was investigated using different parameters such as the effect of contact time, different concentrations of naproxen, the amount of adsorbent and pH. The highest efficiency of naproxen removal was obtained by this adsorbent at pH 6. Also, it was indicated that by increasing the initial concentration of naproxen, contact time and the amount of adsorbent, the efficiency of adsorption process was increased. Based on the experimental results, optimum values of adsorbent dosage, contact time, initial naproxen concentration and pH were evaluated as 1 g, 120 min, 10 mg/l and 6, respectively. Also, the maximum efficiency of adsorption was achieved 92.2%. Experimental data were fitted using nine different isotherms. The results showed that the experimental data were well fitted with all were chosen isotherms except Langmuir and Tempkin, and maximum adsorption capacity was obtained approximately 1.1 mg/g of adsorbent. The positive effect of increasing the initial naproxen concentration on the removal efficiency was proved by Ellovich kinetic model. Generally, the results obtained from this research showed that this adsorbent has a great ability for the removal of naproxen from aqueous solutions.

Table 5
Error functions to evaluate the fit of the nonlinear equation.

Error functions	Equation
Residual root mean square error (*RMSE*)	$\mathrm{RMSE} = \sqrt{\frac{1}{n-2}\sum_{i=1}^{n}(Y_{exp}-Y_{cal})^2}$
The coefficient of determination (R^2)	$R^2 = \frac{(Y_{exp}-\overline{Y}_{cal})^2}{\sum_{i=1}^{n}(Y_{exp}-\overline{Y}_{cal})^2+(Y_{exp}-Y_{cal})^2}$
The sum of the square of the error (*SSE*)	$SSE = \sum_{i=1}^{n}(Y_{exp}-Y_{cal})^2$
The sum of the absolute error (*SAE*)	$SAE = \sum_{i=1}^{n}\lvert Y_{cal}-Y_{exp}\rvert_i$
Average relative error (*ARE*)	$ARE = \frac{1}{n}\sum_{i=1}^{n}\lvert\frac{Y_{cal}-Y_{exp}}{Y_{exp}}\rvert$
The average relative standard error (*ARS*)	$\mathrm{ARS} = \sqrt{\frac{\sum_{i=1}^{n}(Y_{cal}-Y_{exp}/Y_{exp})^2}{n-1}}$
Nonlinear chi-square (χ^2)	$\chi^2 = \sum_{i=1}^{n}\frac{(Y_{cal}-Y_{exp})^2}{Y_{exp}}$
The Correlation coefficient (r)	$r = \frac{n(\sum xy)-(\sum x)(\sum y)}{\sqrt{[n\sum x^2-(\sum x)^2][n\sum y^2-(\sum y)^2]}}$

Acknowledgements

The authors greatly acknowledge Shahid Sadoughi University of Medical Sciences for the financial support from the Grant Research Council.

References

[1] T.A. Ternes, Occurrence of drugs in German sewage treatment plants and rivers, Water Res. 32 (1998) 3245–3260.
[2] T.A. Ternes, M. Bonerz, T. Schidt, Determination of neutral pharmaceuticals in wastewater and rivers by liquid chromatography–electrospray tandem mass spectrometry, J. Chromatogr. A 938 (2001) 175–185.
[3] M. Farre, I. Ferrer, A. Ginebred, M. Figueras, L. Olivella, L. Tirapu, M.D. Vilanova, Barcelo, determination of drugs in surface water and wastewater samples by liquid chromatography-mass spectrometry: methods and preliminary results including toxicity studies with *Vibrio fischeri*, J. Chromatogr. A 938 (2001) 187–197.
[4] I. Rodrıguez, J.B. Quintana, J. Carpinteiro, A.M. Carro, R.A. Lorenzo, R. Cela, Determination of acidic drugs in sewage water by gas chromatography mass spectrometry as tert-butyldimethylsilyl derivatives, J. Chromatogr. A 985 (2003) 265–274.
[5] I. Rodrıguez, J. Carpinteiro, J.B. Quintana, A.M. Carro, R.A. Lorenzo, R. Cela, Solid-phase microextraction with on-fiber derivatization for the analysis of anti-inflammatory drugs in water samples, J. Chromatogr. A 1024 (2004) 1–8.
[6] C. Gonzalez-Barreiro, M. Lores, M.C. Cassis, R. Cela, Simultaneous determination of neutral and acidic pharmaceuticals in wastewater by high-performance liquid chromatography-post-column photochemically induced fluorimetry, J. Chromatogr. A 993 (2003) 29–37.
[7] B. Petrie, R. Barden, B. Kasprzyk-Hordern, A review on emerging contaminants in wastewaters and the environment: current knowledge, understudied areas and recommendations for future monitoring, Water Res. 2014 (2015) 1–25.
[8] M. Devaraj, R. Saravanan, R.K. Deivasigamani, V.K. Gupta, F. Gracia, S. Jayadevan, Fabrication of novel shape Cu and Cu/Cu2O nanoparticles modified electrode for the determination of dopamine and paracetamol, J. Mol. Liq. 221 (2016) 930–941.
[9] United States Pharmacopeia National Formulary, USP 26, NF 21, United States Pharmacopeia National Formulary, Rockville, 2003 1273.
[10] S.F. Webb, A data based perspective on the environmental risk assessment of human pharmaceuticals II aquatic risk characterization, in: K. Ku¨mmerer (Ed.), Pharmaceuticals in the Environment Sources, Fate, Effects and Risks, Springer-Verlag, Berlin, Heidelberg, Germany 2001, pp. 203–219.
[11] D.R. Dietrich, S.F. Webb, T. Petry, Hot spot pollutants: pharmaceuticals in the environment, Toxicol. Lett. 131 (2002) 1–3.

Table 6
Isotherms error function data related to naproxen onto nanocomposite adsorbent.

Isoterm model	*SSE*	*SAE*	*ARE*	*ARS*	*RMSE*	r	χ^2	R^2
Langmuir	0.1830	1.1258	4.8072	0.6438	0.6787	0.9025	0.7227	0.8145
Froundlich	0.1657	0.7178	4.1092	0.6326	0.2108	0.9241	0.6512	0.9539
Tempkin	6.0020	5.0887	46.7747	8.8615	9.3409	0.9370	56.333	0.8745
Fritz–Schlunder	0.1432	0.7188	3.1604	0.6326	0.6668	0.9208	0.6512	0.9480
Redlich-peterson (P-R)	0.1432	0.7188	4.1104	0.6326	0.6668	0.9208	0.6512	0.9480
Radke–Prausnitz (R-P)	0.1432	0.7188	3.1606	0.6326	0.6668	0.9208	0.6512	0.9480
Sips	0.1433	0.7202	4.1132	0.6326	0.6668	0.9208	0.6513	0.9479
Toth	0.1432	0.7188	4.1103	0.6326	0.6668	0.9210	0.6512	0.9483
Khan	0.1432	0.7190	4.1108	0.6326	0.6668	0.9208	0.6512	0.9480

[12] M.N. Chong, B. Jin, Photocatalytic treatment of high concentration carbamazepine in synthetic hospital wastewater, J. Hazard. Mater. 199 (2012) 135–142.
[13] P. Westerhoff, Removal of endocrine disruptors, pharmaceuticals, and personal care products during water treatment, Southwest Hydrol. 2 (2003) 18–19.
[14] R. Rostamian, M. Najafi, A.A. Rafati, Synthesis and characterization of thiol-functionalized silica nano hollow sphere as a novel adsorbent for removal of poisonous heavy metal ions from water: kinetics, isotherms and error analysis, Chem. Eng. J. 171 (2011) 1004–1011.
[15] L. Rafati, R. Nabizade, A.H. Mahvi, M.H. Dehghani, Removal of phosphate from aqueous solutions by iron nano particle resin lewatit (FO36), Korean J. Chem. Eng. 29 (2012) 473–477.
[16] M. Najafi, Y. Yousefi, A.A. Rafati, Synthesis, characterization and adsorption studies of several heavy metal ions on amino-functionalized silica nano hollow sphere and silica gel, Sep. Purif. Technol. 85 (2012) 193–205.
[17] V.K. Gupta, D. Pathania, S. Sharma, S. Agarwal, P. Singh, Remediation of noxious chromium (VI) utilizing acrylic acid grafted lignocellulosic adsorbent, J. Mol. Liq. 177 (2013) 343–352.
[18] M.S. Karmacharya, V.K. Gupta, I. Tyagi, S. Agarwal, V.K. Jha, Removal of As (III) and As (V) using rubber tire derived activated carbon modified with alumina composite, J. Mol. Liq. 216 (2016) 836–844.
[19] T.A. Saleh, V.K. Gupta, Column with CNT/magnesium oxide composite for lead (II) removal from water, Environ. Sci. Pollut. Res. 19 (2012) 1224–1228.
[20] V.K. Gupta, S.K. Srivastava, D. Mohan, S. Sharma, Design parameters for fixed bed reactors of activated carbon developed from fertilizer waste for the removal of some heavy metal ions, Waste Manag. 17 (1998) 517–522.
[21] A. Mittal, J. Mittal, A. Malviya, D. Kaur, V.K. Gupta, Decoloration treatment of a hazardous triarylmethane dye, Light Green SF (Yellowish) by waste material adsorbents, J. Colloid Interface Sci. 342 (2010) 518–527.
[22] A. Mittal, D. Kaur, A. Malviya, J. Mittal, V.K. Gupta, Adsorption studies on the removal of coloring agent phenol red from wastewater using waste materials as adsorbents, J. Colloid Interface Sci. 337 (2009) 345–354.
[23] A. Mittal, J. Mittal, A. Malviya, V.K. Gupta, Adsorptive removal of hazardous anionic dye "Congo red" from wastewater using waste materials and recovery by desorption, J. Colloid Interface Sci. 340 (2009) 16–26.
[24] V.K. Gupta, S. Agarwal, T.A. Saleh, Synthesis and characterization of alumina-coated carbon nanotubes and their application for lead removal, J. Hazard. Mater. 185 (2011) 17–23.
[25] V.K. Gupta, I. Ali, T.A. Saleh, A. Nayak, S. Agarwal, Chemical treatment technologies for waste-water recycling—an overview, RSC Adv. 2 (2012) 6380–6388.
[26] A. Mittal, J. Mittal, A. Malviya, V.K. Gupta, Removal and recovery of Chrysoidine Y from aqueous solutions by waste materials, J. Colloid Interface Sci. 344 (2010) 497–507.
[27] V.K. Gupta, R. Jain, A. Nayak, S. Agarwal, M. Shrivastava, Removal of the hazardous dye—tartrazine by photodegradation on titanium dioxide surface, Mater. Sci. Eng. C 31 (2011) 1062–1067.
[28] V.K. Gupta, A. Nayak, Cadmium removal and recovery from aqueous solutions by novel adsorbents prepared from orange peel and Fe2O3 nanoparticles, Chem. Eng. J. 180 (2012) 81–90.
[29] T.A. Saleh, V.K. Gupta, Photo-catalyzed degradation of hazardous dye methyl orange by use of a composite catalyst consisting of multi-walled carbon nanotubes and titanium dioxide, J. Colloid Interface Sci. 371 (2012) 101–106.
[30] H. Khani, M.K. Rofouei, P. Arab, V.K. Gupta, Z. Vafaei, Multi-walled carbon nanotubes-ionic liquid-carbon paste electrode as a super selectivity sensor: application to potentiometric monitoring of mercury ion (II), J. Hazard. Mater. 183 (2010) 402–409.
[31] S. Karthikeyan, V.K. Gupta, R. Boopathya, A. Titusa, G. Sekaran, A new approach for the degradation of high concentration of aromatic amine by heterocatalytic Fenton oxidation: kinetic and spectroscopic studies, J. Mol. Liq. 173 (2012) 153–163.
[32] L.A. Belyakova, K.A. Kazdobin, V.N. Belyakov, S.V. Ryabov, A.F. Danil de Namor, Synthesis and properties of supra-molecular systems based on silica, J. Colloid Interface Sci. 283 (2005) 488–494.
[33] A.K. Jain, V.K. Gupta, A. Bhatnagar, Suhas, A comparative study of adsorbents prepared from industrial wastes for removal of dyes, Sep. Sci. Technol. 38 (2003) (2007) 463–481.
[34] V.K. Gupta, A. Nayak, S. Agarwal, Bioadsorbents for remediation of heavy metals: current status and their future prospects, Environ. Eng. Res. 20 (2015) 001–018.
[35] F. Gode, E. Pehlivan, A comparative study of two chelating ion-exchange resins for the removal of chromium (III) from aqueous solution, J. Hazard. Mater. 100 (2003) 231–243.
[36] T.A. Saleh, V.K. Gupta, Processing methods, characteristics and adsorption behavior of tire derived carbons: a review, Adv. Colloid Interf. Sci. 211 (2014) 93–101.
[37] V.K. Gupta, A. Mittal, D. Jharec, J. Mittal, Batch and bulk removal of hazardous colouring agent Rose Bengal by adsorption techniques using bottom ash as adsorbent, RSC Adv. 2 (2012) 8381–8389.
[38] S. Han James, N. Hur, B. Choi, S.H. Min, Removal of phosphorus using chemically modified lignocellulosic materials, 6th Inter-regional Conference on Environment-water Land and Water Use Planning and Management, Albacete, Spain, September 3–5, 2003.
[39] V.K. Gupta, R. Kumar, A. Nayak, T.A. Saleh, M.A. Barakat, Adsorptive removal of dyes from aqueous solution onto carbon nanotubes: a review, Adv. Colloid Interf. Sci. 193-194 (2013) 24–34.
[40] R. Saravanan, E. Sacari, F. Gracia, M.M. Khan, E. Mosquera, V.K. Gupta, Conducting PANI stimulated ZnO system for visible light photocatalytic degradation of coloured dyes, J. Mol. Liq. 221 (2016) 1029–1033.
[41] A. El Nemr, Potential of pomegranate husk carbon for Cr (VI) removal from wastewater: kinetic and isotherm studies, J. Hazard. Mater. 161 (2009) 132–141.
[42] S. Rajendran, M.M. Khan, F. Gracia, J. Qin, V.K. Gupta, S. Arumainathan, Ce^{3+} ion-induced visible-light photocatalytic degradation and electrochemical activity of ZnO/CeO_2 nanocomposite, Sci. Rep. 6 (2016) 31641.
[43] R. Saravanan, V.K. Gupta, E. Mosquera, F. Gracia, V. Narayanan, A. Stephen, Visible light induced degradation of methyl orange using β-Ag0.333V2O5 nanorod catalysts by facile thermal decomposition method, J. Saudi Chem. Soc. 19 (2015) 521–527.
[44] R. Saravanan, F. Gracia, M.M. Khan, V. Poornima, V.K. Gupta, V. Narayanan, A. Stephen, ZnO/CdO nanocomposites for textile effluent degradation and electrochemical detection, J. Mol. Liq. 209 (2015) 374–380.
[45] Y.S. Ho, G. McKay, Pseudo-second order model for sorption processes, Process Biochem. 34 (1999) 451–465.
[46] R. Saravanan, M.M. Khan, V.K. Gupta, E. Mosquera, F. Gracia, V. Narayanan, A. Stephen, ZnO/Ag/Mn2O3 nanocomposite for visible light-induced industrial textile effluent degradation, uric acid and ascorbic acid sensing and antimicrobial activity, RSC Adv. 5 (2015) 34645–34651.
[47] R. Saravanan, M.M. Khan, V.K. Gupta, E. Mosquera, F. Gracia, V. Narayanan, A. Stephen, ZnO/Ag/CdO nanocomposite for visible light-induced photocatalytic degradation of industrial textile effluents, J. Colloid Interface Sci. 452 (2015) 126–133.
[48] R. Saravanan, V.K. Gupta, V. Narayanan, A. Stephen, Visible light degradation of textile effluent using novel catalyst ZnO/γ-Mn2O3, J. Taiwan Inst. Chem. Eng. 45 (2014) 1910–1917.
[49] Y.S. Ho, C.C. Chiang, Y.C. Hsu, Sorption kinetics for dye removal from aqueous solution using activated clay, Sep. Sci. Technol. 36 (2001) 2473–2488.
[50] R. Saravanan, V.K. Gupta, E. Mosquera, F. Gracia, Preparation and characterization of V2O5/ZnO nanocomposite system for photocatalytic application, J. Mol. Liq. 198 (2014) 409–412.
[51] R. Saravanan, T. Prakashc, V.K. Gupta, A.S. Tailorin, The electrical and dielectric properties of ZnO nanorods by substitution, J. Mol. Liq. 193 (2014) 160–165.
[52] R.S. Juang, M.L. Chen, Application of the Elovich equation to the kinetics of metal sorption with solvent-impregnated resins, Ind. Eng. Chem. 36 (1997) 813–820.
[53] R. Saravanan, N. Karthikeyan, V.K. Gupta, E. Thirumal, P. Thangadurai, V. Narayanan, A. Stephen, ZnO/Ag nanocomposite: an efficient catalyst for degradation studies of textile effluents under visible light, Mater. Sci. Eng. C 33 (2013) 2235–2244.
[54] R. Saravanan, V.K. Gupta, V. Narayanan, A. Stephen, Comparative study on photocatalytic activity of ZnO prepared by different methods, J. Mol. Liq. 181 (2013) 133–141.
[55] M.J.D. Low, Kinetics of chemisorption of gases on solids, Chem. Rev. 60 (1960) 267–312.
[56] R. Saravanan, S. Joicy, V.K. Gupta, V. Narayanan, A. Stephen, Visible light induced degradation of methylene blue using CeO2/V2O5 and CeO2/CuO catalysts, Mater. Sci. Eng. C 33 (2013) 4725–4731.
[57] R. Saravanan, S. Karthikeyan, V.K. Gupta, G. Sekaran, V. Narayanan, A. Stephen, Enhanced photocatalytic activity of ZnO/CuO nanocomposite for the degradation of textile dye on visible light illumination, Mater. Sci. Eng. C 33 (2013) 91–98.
[58] F. Colak, N. Atar, A. Olgun, Biosorption of acidic dyes from aqueous solution by *Paenibacillus macerans*: kinetic, thermodynamic and equilibrium studies, J. Chem. Eng. 150 (2009) 122–130.
[59] R. Saravanan, E. Thirumal, V.K. Gupta, V. Narayanan, A. Stephen, The photocatalytic activity of ZnO prepared by simple thermal decomposition method at various temperatures, J. Mol. Liq. 177 (2013) 394–401.
[60] R. Saravanan, V.K. Gupta, T. Prakash, V. Narayanan, A. Stephen, Synthesis, characterization and photocatalytic activity of novel Hg doped ZnO nanorods prepared by thermal decomposition method, J. Mol. Liq. 178 (2013) 88–93.
[61] H. Lee, D.S. Kim, Preparation and physical properties of wood/polypropylene/clay, nanocomposites, 111 (2009) 2769–2776.
[62] C. Ravindra Reddy, A. Pouyan Sardashti, L.C. Simon, Preparation and characterization of polypropylene–wheat straw–clay composites, Compos. Sci. Technol. 70 (2010) 1674–1680.
[63] L. Rafati, A.H. Mahvi, A.R. Asgari, S.S. Hosseini, Removal of chromium (VI) from aqueous solutions using Lewatit FO36 nano ion exchange resin, Int. J. Environ. Sci. Technol. 7 (2010) 147–156.
[64] V.K. Gupta, T.A. Saleh, Sorption of pollutants by porous carbon, carbon nanotubes and fullerene- an overview, Environ. Sci. Pollut. Res. 20 (2013) 2828–2843.
[65] T.A. Saleh, V.K. Gupta, Functionalization of tungsten oxide into MWCNT and its application for sunlight-induced degradation of rhodamine B, J. Colloid Interface Sci. 362 (2011) 337–344.
[66] J.R. Domínguez-Vargas, T. Gonzalez, P. Palo, E.M. Cuerda-Correa, Removal of carbamazepine, naproxen, and trimethoprim from water by Amberlite XAD-7: a kinetic study, Clean: Soil, Air, Water 41 (2013) 1052–1061.
[67] Z. Yu, S. Peldszus, P.M. Huck, Adsorption of selected pharmaceuticals and an endocrine disrupting compound by granular activated carbon. 2. Model prediction, Environ. Sci. Technol. 43 (2009) 1474–1479.
[68] L.M. Madikizela, L. Chimuka, Synthesis, adsorption and selectivity studies of a polymer imprinted with naproxen, ibuprofen and diclofenac, J. Environ. Chem. Eng. 4 (2016) 4029–4037.
[69] R. Baccar, M. Sarrà, J. Bouzid, M. Feki, P. Blánquez, Removal of pharmaceutical compounds by activated carbon prepared from agricultural by-product, Chem. Eng. J. 211–212 (2012) 310–317.
[70] Z. İlbay, S. Şahin, Ö. Kerkez, Ş.S. BayazitEmail, Isolation of naproxen from wastewater using carbon-based magnetic adsorbents, Int. J. Environ. Sci. Technol. 12 (2015) 3541–3550.
[71] Z. Hasan, J. Jeon, S.H. Jhung, Adsorptive removal of naproxen and clofibric acid from water using metal-organic frameworks, J. Hazard. Mater. 209–210 (2012) 151–157.
[72] S.M. Rivera-Jiménez, S. Méndez-González, A. Hernández-Maldonado, Metal (M = Co^{2+}, Ni^{2+}, and Cu^{2+}) grafted mesoporous SBA-15: effect of transition metal

incorporation and pH conditions on the adsorption of naproxen from water, Microporous Mesoporous Mater. 132 (2010) 470–479.
[73] Y. Önal, C. Akmil-Başar, Ç. Sarıcı-Özdemir, Elucidation of the naproxen sodium adsorption onto activated carbon prepared from waste apricot: kinetic, equilibrium and thermodynamic characterization, J. Hazard. Mater. 148 (2007) 727–734.
[74] T.A. Saleh, V.K. Gupta, Column with CNT/magnesium oxide composite for lead (II) removal from water, Environ. Sci. Pollut. Res. 19 (2012) 1224–1228.
[75] V.K. Gupta, R. Jain, A. Mittal, T.A. Saleh, A. Nayak, S. Agarwal, S. Sikarwar, Photo-catalytic degradation of toxic dye amaranth on TiO_2/UV in aqueous suspensions, Mater. Sci. Eng. C 32 (2012) 12–17.
[76] W.S. Wan Ngah, M.A.K.M. Hanafiah, Adsorption of copper on rubber (*Hevea brasiliensis*) leaf powder: kinetic, equilibrium and thermodynamic studies, Biochem. Eng. J. 39 (2008) 521–530.